A New Position and Speed Estimation Scheme for Position Control of PMSM Drives Using Low-resolution Position Sensors

Qinan Ni, Ming Yang, *Senior Member*, *IEEE*, Shafiq Ahamed Odhano, Mi Tang, Pericle Zanchetta, *Fellow*, *IEEE*, Xiaosheng Liu and Dianguo Xu, *Fellow*, *IEEE*

***Abstract*—A new position control method for PMSM drive with a low-resolution encoder is proposed in this paper. Three binary Hall position sensors are utilized to realize a moderate-performance position control system for the consideration of economy and simplicity in servo application. Compared with sensorless control, the usage of binary Hall position sensors is a guarantee of both control performance and low cost. However, the low resolution of Hall sensor will heavily deteriorate the accuracy of the position and speed calculation. Such drawback can be effectively minimized by using appropriate positon and speed estimation schemes. With the help of polynomial fitting and state observer techniques, a solution is provided to realize semi-closed loop control by treating the position and speed estimators as separate systems. The performance can be improved (1) by proposing a polynomial fitting scheme with least squares (LS) method, high-resolution rotor-position predictor can be derived by fitting the predefined position data from binary Hall position sensors in a linear or quadratic manner; (2) by adopting the dual-sampling-rate observer, instantaneous speed can be estimated at each control cycle and the estimation error is corrected once a new measurement form the Hall arrives. Furthermore, a nonlinear position control algorithm is introduced to increase standstill stability. Extensive experimental results are given to demonstrate the feasibility of the proposed method and its superiority over conventional methods.**

***Index Terms*—Binary Hall position sensors, least squares (LS), polynomial fitting, dual-sampling-rate observer, position control.**

I. Introduction

THE surface-mounted permanent magnet synchronous machine (SPMSM) has become the main trend for AC servo application due to merits, e.g. high efficiency, small volume and compact structure, etc. AC servo motor drives based on field-oriented control (FOC) is dominant in position control systems, whose performance mainly depends on the accuracy of rotor position and speed feedbacks [1]. Generally, cost and reliability are the primary concern for industrial applications, such as machine tools, automotive industry, electric vehicles, and home appliances, where sometimes the practical working conditions are harsh and unfriendly to high resolution encoder. In this sense, many position sensorless techniques have been developed to realize sensorless control of SPMSM drive in the wide speed range over the last two decades or so [2-4]. However, the dynamic response is not fast enough when using most of those methods, and the position control has been rarely considered. In addition, it is well known that most of the sensorless methods are still not mature to guarantee the desired performance within wide speed and torque range for some mission-critical drives [5].

Meanwhile, as a practical compromise, the sensor board fixed to the stator including inexpensive binary Hall sensors (<$2) is often employed since it requires very little cost and volume in comparison with shaft-mounted sensors. While it can still provide discrete absolute rotor position information [6, 7]. However, due to the extremely low resolution, the position error will be inevitably large if Hall sensors' signals are directly used, which will also worsen the current control performance. In this respect, the choice of a decent estimator to get the accurate speed and the high resolution position for satisfactory operation of motors in a given application is one of the key issues in Hall sensors based drives.

In recent years, a lot of investigations on PMSM drives using binary Hall sensors have been done and two major solutions have been extensively studied in the literatures to achieve high precision position and speed estimation which are commonly referred as "estimation methods" [8].

The first solution is *non-model-based*, which generally exploits signal processing technologies. Various kinds of data processing methods can be found in the literatures, such as the methods based on first or high order approximations, polynomial interpolation, least square interpolation on position trajectory, and linear or nonlinear numerical integrations [9-13]. These methods predict the subsequent rotor position by using the polynomial equation to approximate the previous rotor movement profile without using any model parameters. After the position information is calculated, the speed can easily be estimated using numerical differentiation methods. From a mathematical point of view, it is equivalent to the problem of determining a continuous, and thus differentiable, function that interpolates the quantized discontinuous position measurement

Manuscript received November 05, 2018; revised January 23, 2019 and March 05; accepted March 06, 2019. Paper 2018-IDC-1095. R2, presented at the 2018 Energy Conversion Congress and Exposition, Portland, OR, USA, Sep. 23-27, and approved for publication in the IEEE Transactions on Industry Applications by the Industrial Drives Committee of the IEEE Industry Applications Society. This work was supported by the Delta Environmental & Educational Foundation (DREM2017004).

Q. Ni, M. Yang, X. Liu, D. Xu are the School of Electrical Engineering and Automation, Harbin Institute of Technology, Harbin 150001, China (e-mail: niqn_hit@163.com; yangming@hit.edu.cn; liuxsh@hit.edu.cn; xudiang@hit.edu.cn).

S. A. Odhano, M. Tang, P. Zanchetta are the Department of Electrical and Electronic Engineering, University of Nottingham, Nottingham NG7 2RD, U. K. (email: shafiq.odhano@nottingham.ac.uk; Mi.Tang2@nottingham.ac.uk; pericle.zanchetta@nottingham.ac.uk.)

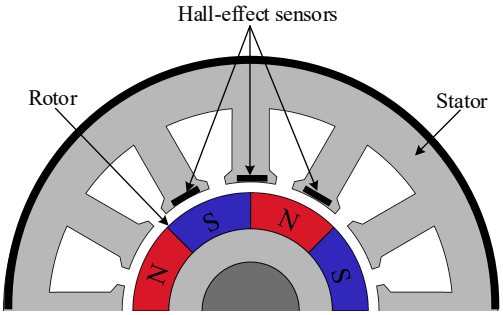

Fig. 1. Surface-mounted PMSM for servo applications and binary Hall sensors installation in the stator.

[11]. These methods, by way of signal processing, are relatively simple for implementation. However, the problem of time delay and spike in estimated speed is unavoidable, and thus the error in speed estimation may result in slower, inefficient, and sometimes even unstable motions.

The other solutions such as state observers [14-18] and Kalman filters [19, 20] are *model-based* technology which require the information of the model (e.g., mechanical and electrical models) and the measurements of the other necessary variables in a motor drive system (e.g., DC-link voltage measurement and current measurements. The state observers based on Luenberger structure that need mechanical parameters and motor torque were introduced in [15]. This estimation method takes advantage of the information of mechanical model and features high-accuracy and good dynamic characteristics in speed estimation. However, it should be noted that, the performance of the observer depends heavily on the quality of the observer input (e.g., position measurement from Hall sensors) and the accuracy of the mechanical parameters [6,16]. So, bumps may exist in speed observation due to the position error from the quantization in the Hall sensors based drives, and performance degradation of the observers is unavoidable if there exist changes in mechanical parameters [17]. Furthermore, the rotor position information in such method is usually acquired from the estimated speed using numerical integration. Hence, the estimated speed error can affect the position estimation directly, so it limits the overall performance of servo motor drive with cascaded-loop control structure, especially during start-up, low speed, and speed reversal operations. Others such as [18] proposed the back electromotive force estimation scheme to estimate the speed and use the Hall signals to limit the estimation error at the start-up and low speed operations, but it depends on current measurements and the accuracy of electrical parameters. Moreover, current derivatives are not easy to calculate precisely without considering the nonlinearities of the inverter. Strategies based on Kalman filters usually need to know the noise variance and assume that the quantization error is as Gaussian noise, which is hard to be satisfied in practice.

Motivated by the aforementioned analyses, in order to fulfill a moderate motion control performance in Hall sensors based motor drives, the dynamic response of speed estimation should be fast enough to fit into a high-bandwidth control loop. Also, the position estimation should be smooth enough to avoid torque ripple and undesired oscillations in the loops. However,

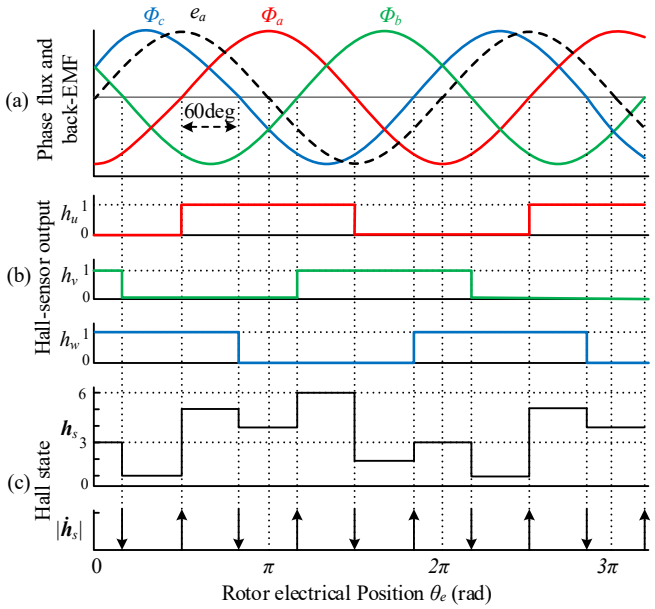

Fig. 2. Air gap flux and processed signals of binary Hall sensors.

the two opposite goals in position and speed estimation cannot be achieved in one estimation at the same time. Since *non-model-based* methods can smoothly process the quantized Hall position signal and the *model-based* methods feature good dynamics in speed estimation by taking advantage of model information, it is reasonable to design the position and speed estimators separately by taking the advantages of those *non-model-based* and *model-based* methods [13,21,22].

To solve the problems analyzed above in the existing researches, an improved rotor position and speed estimation method for SPMSM drive system with low-resolution binary Hall position sensors is presented in this paper, which also adopts the non-linear position controller in the position loop to improve system stability. More concretely: 1) the position signal is approximated by least-squares polynomial fitting method based on sets of position measurements, and the estimation error appearing in speed reversal operation is compensated by using the plant model; 2) a Luenberger style dual-sampling-rate observer with motor torque as a feedforward input term is built to achieve high accuracy and high bandwidth speed estimation, which can output the instantaneous speed at each control cycle and correct the estimation error whenever the Hall measurements change; 3) a non-linear position controller is adopted to control the motor shaft position so that an acceptable and reliable control can be obtained in position control applications. Compared with the existing methods, as such, in the presence of position control, the proposed method adopts least squares polynomial fitting algorithm. Since it is an open-loop rotor position estimation strategy, it does not need injected signals or modifying PWM switching patterns compared with the traditional position sensorless techniques, and it does not require parameters of the motor and back EMF compared with the model based Hall sensors position estimator. Besides, estimation error is compensated to make the proposed method suitable in multiple operation conditions. In the

presence of speed estimation, bump which is caused by the discretization of Hall sensors is best reduced, favorable transient performance is realized and the proposed method has the least parameters requirement compared to state of the art. Moreover, the adoption of non-linear position controller realizes closed-loop position control and avoid the speed oscillation at standstill.

This paper is organized as follows. In Section II, the system with three binary Hall sensors is introduced, and the operation principle of the binary Hall sensor is described. In Section III, the performance limitations of two conventional estimation methods are analyzed from the perspectives of time delay and estimation errors. In Section IV, the proposed scheme is introduced in detail, followed by observer tuning and performance analysis. The experimental results confirm the effectiveness of the proposed method in Section V. Section VI concludes the whole paper.

II. Analysis of Binary Hall Position Sensors Based PMSM Drive System

Three Hall elements are employed to recognize the rotor absolute position in the drive system, as shown in Fig. 1. The three Hall sensors can generate absolute rotor position information with a resolution of ± 30° electrical angle.

Fig. 1 shows a simplified cross-sectional view of a 750W surface-mounted 8 poles/12 slots SPMSM that is applied to servo application, wherein the SPM has an outer stator and inner rotor structure with a concentrated winding; the three Hall sensors Hu, Hv, Hw are included in the sensor board for the detection of the N-pole and S-pole of the permanent magnet, thus they generate square-wave voltage outputs.

The signals generated by Hall sensors in our system will lag each other by 120° as the 120° type mechanical installation is adopted. Fig. 2 (a) shows the three phase flux (Φ_a, Φ_b, Φ_c) and back EMF (e_a, e_b, e_c) waveform at steady state. Fig. 2 (b) depicts the corresponding output signals (h_u, h_v, h_w) produced by three Hall sensors which are displaced by 120° electrical. Fig. 2 (c) shows the Hall vector $\boldsymbol{h}_s$ which represents the binary expression of three Hall sensors states; $\left|\dot{\boldsymbol{h}}_s\right|$ denotes the Hall signal pulse verge which can be used to revise the angle output in different direction, e.g., the Hall vector $\boldsymbol{h}_s$ outputs 1 both in clockwise (CW) and counter clockwise (CCW), but the actual rotor position is π/6 and π/2 respectively.

III. Performance Limitation Analysis of Conventional Methods

Two common position and speed estimation methods, i.e. average speed method and Luenberger observer method, are analyzed in the following subparagraphs. The analysis shows that the two methods may introduce time delay and errors in the estimated position and speed, and this can influence the dynamic and steady performances as well as the stability of whole system.

A. Average speed method

The average speed method is an effective and straightforward way to measure rotor speed for low-count encoder system

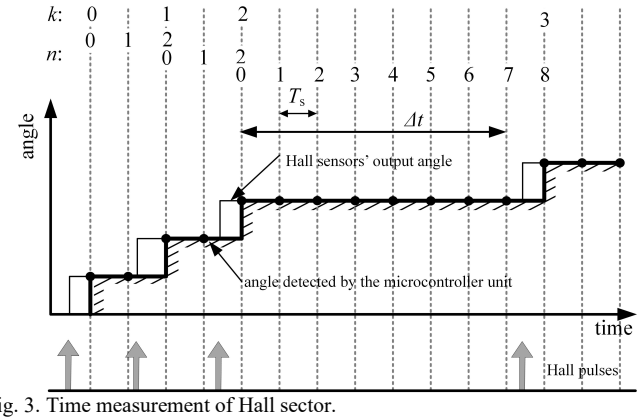

Fig. 3. Time measurement of Hall sector.

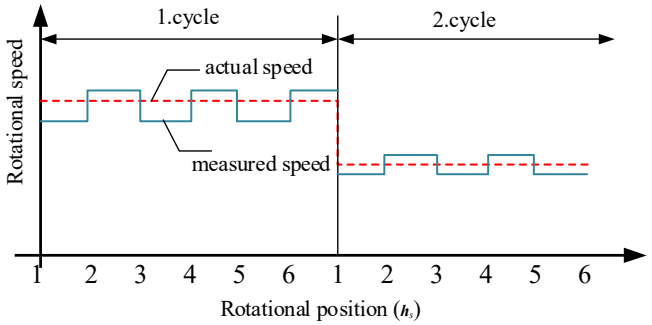

Fig. 4. Actual rotational speed and calculated average rotational speed

which only needs the measurement of time between the last two Hall verges, Fig. 3. The speed is calculated by the following expression if the speed is assumed to be a constant:

$$\omega_{avg}(t_k)=\frac{\Delta\theta_k}{\Delta t_k}=\frac{\theta_k-\theta_{k-1}}{P\cdot n\cdot T_s} \tag{1}$$

where Δt is the time interval of Hall sector, $\theta(k)$ is the kth quantized position measured from the Hall sensors at time instant t_k, ω_{avg} is the calculated rotor speed, P is the motor pole pairs, T_s is the sampling period of the digital control system. The sampling instant $[k, n]$ is defined by

$$t=\sum_{a=0}^{k}T_1(\theta(t_a))+nT_s=[k,n] \tag{2}$$

where k denotes the sample numbers of the Hall signal, and n indicates the sample numbers of control period, respectively.

From the formula, an estimated speed can be calculated for only once at each period of the Hall signals. Thus, the speed sampling period (T_1) increases as motor speed decreases. As a result, the accuracy of the estimation not only depends on the rotor running condition during each Hall sector, but also on the ratio between the sampling period of control cycle and that of the calculated speed. For example, as shown in Fig. 4, when machine rotates at constant speed, due to the inaccuracy in the detected position, Δt may exit $\pm T_s$ sampling error and the calculated speed by (1)has an error, which is roughly linear with actual speed:

$$e_\omega\%=\frac{T_s}{2\pi/6\cdot\omega_e-T_s}\cong\frac{\omega_e\cdot 6\cdot T_s}{2\pi} \tag{3}$$

The error in estimated speed can affect the control performance of both speed loop and current loop if the rotor position is from the numerical integration of the average speed as:

$$\hat{\theta}_{avg}(t_{k+n})=\frac{1}{t_{k-1}-t_k}\{(\theta_{k-1}-\theta_k)\cdot(t_k+n\cdot T_s)+\theta_k\cdot t_{k-1}-\theta_{k-1}\cdot t_{k-1}\} \tag{4}$$

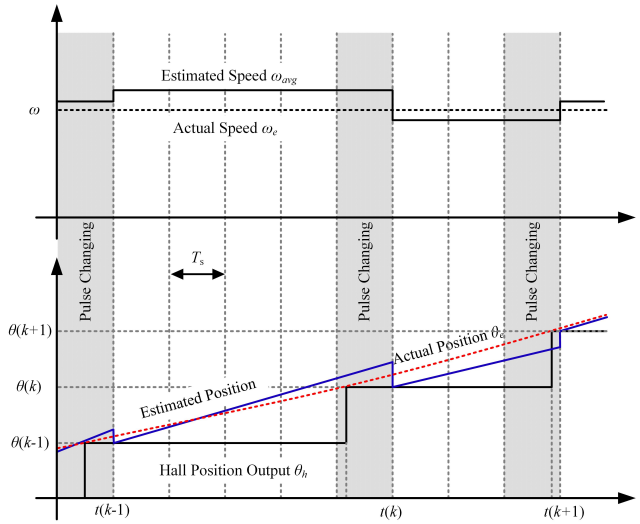

Fig. 5. Position estimation result with average speed method

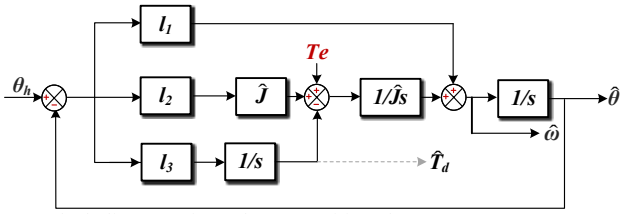

Fig. 6. Block diagram of Luenberger position observer

where $k+n$ denotes the present moment. The resultant interpolated position by (4) has the discontinuity wherever the Hall signal occurs even at constant speed, as shown in Fig. 5.

To reduce the discontinuity of the calculated speed from average speed method, the simplest solution is adopting the moving average (MA) filter for the past N samples, whose expression is give as:

$$F(s)=\frac{1}{N}\sum_{i=0}^{N-1}e^{-si\Delta t} \tag{5}$$

Then, applying Laplace transform to (1), the transfer function between the filtered and actual velocity can be described as:

$$\begin{aligned}H(s)&=\frac{\hat{\Omega}(s)}{\Omega(s)}\approx\frac{1-e^{-s\Delta t}}{s\Delta t}\cdot\frac{1}{N}\sum_{i=0}^{N-1}e^{-si\Delta t}\\&=\frac{1}{sN\Delta t}\sum_{i=0}^{N-1}(e^{-s\Delta t}-e^{-s(i+1)\Delta t})\\&=\frac{1}{sN\Delta t}\left(\underbrace{1-e^{-s\Delta t}}_{i=0}+\underbrace{e^{-s\Delta t}-e^{-s2\Delta t}}_{i=1}+\cdots+\underbrace{e^{-s(N-1)\Delta t}-e^{-sN\Delta t}}_{i=N-1}\right)\\&=\frac{1-e^{-sN\Delta t}}{sN\Delta t}\end{aligned} \tag{6}$$

where magnitude and phase can be described as follows:

$$\begin{aligned}|H(j\omega)|&=\frac{|\sin(\omega N\Delta t/2)|}{\omega N\Delta t/2}\\\angle H(j\omega)&=-\omega N\Delta t/2\end{aligned} \tag{7}$$

Thus, the estimated speed of average speed method with MA filter acts as a low pass filter whose effects on the velocity are presented in [22]. Due to the delay of the estimated velocity in the low-speed region and the integration error in estimated position, the speed control loop may become slower and inefficient, and sometimes even unstable.

B. *Luenberger observer method*

The speed can be estimated on the basis of mechanical state equations. The method utilizing a Luenberger observer illustrated in Fig. 6 has superior dynamic characteristics and high accuracy in estimation, such observer has intrinsic zero-lag tracking capability.

Neglecting the influence of friction, thus the expression of the observer can be given as

$$\begin{aligned}\dot{\hat{x}}&=A\hat{x}+Bu+L(y-\hat{y})\\\frac{d}{dt}\begin{bmatrix}\hat{\theta}\\\hat{\omega}\\\hat{T}_d\end{bmatrix}&=\begin{bmatrix}0&1&0\\0&0&-1/\hat{J}\\0&0&0\end{bmatrix}\begin{bmatrix}\hat{\theta}\\\hat{\omega}\\\hat{T}_d\end{bmatrix}+\begin{bmatrix}0\\1/\hat{J}\\0\end{bmatrix}T_e+\begin{bmatrix}l_1\\l_2\\l_3\end{bmatrix}\left(\theta_h-\hat{\theta}\right)\end{aligned} \tag{8}$$

where θ_h, T_d, T_e, and J represent quantized Hall position data, load torque, electromagnetic torque, and total rotational inertia (electrical representation), respectively. L is the observer gain. y represents the output variables, and $\hat{y}=C\hat{x}=[1\quad 0\quad 0]\hat{x}$.

The transfer function for the estimated speed, $\hat{\omega}$, can be deduced as follows:

$$\hat{\omega}=\frac{\hat{J}l_1s^3+\hat{J}l_2s^2-l_3s}{\hat{J}s^3+\hat{J}l_1s^2+\hat{J}l_2s-l_3}\theta_h+\frac{s^2}{\hat{J}s^3+\hat{J}l_1s^2+\hat{J}l_2s-l_3}T_e \tag{9}$$

In (9), the quantized Hall position and the torque reference can be written as

$$\theta_h=\frac{1-e^{-s\Delta t}}{s}\theta, T_e=Js\omega. \tag{10}$$

From (10), the transfer function for rotor speed is

$$\hat{\omega}=\frac{Js^3+(\hat{J}l_1s^2+\hat{J}l_2s-l_3)\dfrac{1-e^{-s\Delta t}}{s}}{\hat{J}s^3+\hat{J}l_1s^2+\hat{J}l_2s-l_3}\omega \tag{11}$$

The error of estimation ω can be expressed as

$$\Delta\omega=\omega-\hat{\omega}=\frac{\Delta Js^3+(\hat{J}l_1s^2+\hat{J}l_2s-l_3)(1-\dfrac{1-e^{-s\Delta t}}{s})}{\hat{J}s^3+\hat{J}l_1s^2+Jl_2s-l_3}\omega \tag{12}$$

where $\Delta J=\hat{J}-J$.

From (12), it is clear that the estimated speed error is affected by both Δt and ΔJ. In servo systems, however, the moment of inertia varies slightly in a specific application, and it can be estimated by off-line method, so it can be assumed known. For outputting speed estimation at every control period T_s, observer input θ_h varies in step manner, it can be regarded as a piecewise constant signal during every Hall interval Δt. And Δt is much bigger than T_s almost in the whole speed range when using low-count encoder. Therefore, Δt must be considered, and this is the reason for the existence of bumps [22].

Again, the rotor position is usually obtained by interpolation method instead of the estimated angle $\hat{\theta}$ in the observer. Hence, the estimated rotor speed error can affect the inner current loop and thus the torque regulation, so it limits the system performance and stability.

IV. PROPOSED SCHEME

Fig. 7 exhibits the overall block diagram of the proposed

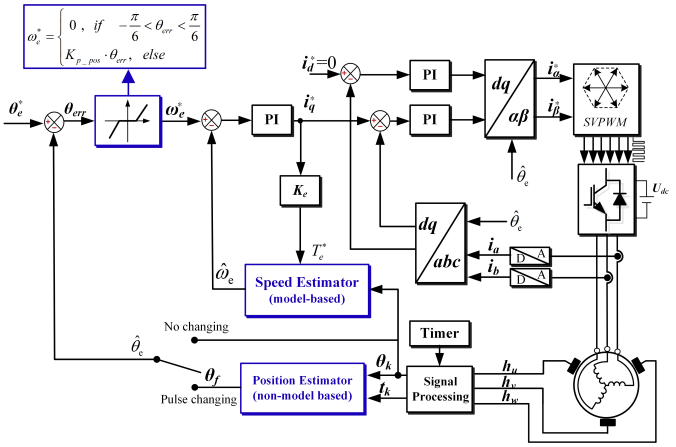

Fig. 7. Overall block diagram of the proposed control strategy for SPMSM drives with Hall sensors

control strategy for SPMSM drives with Hall sensors. Since the least-squares polynomial fitting (LSPF) method can smoothly process the quantized position signal and the observer method has intrinsic zero-lag tracking capability benefit from the plant model information, a new method that combines them together is proposed to estimate the motor position and speed in this paper. The polynomial fitting approach based on least square method is developed to estimate the rotor position, which can produce a smooth estimation output without using plant parameters. Also, a compensation method for position estimator under speed reversal condition is adopted to diminish the estimation error. The Luenberger style dual-sampling-rate reduced-order observer with a feedforward input of motor torque is proposed to estimate the speed. Moreover, the general PI controller is applied to control the speed and current loop, which generates the voltage reference to SVPWM module. Since the traditional P controller which is applied in position loop cannot effectively control the actual position especially when position error varies nonlinearly at standstill, a nonlinear controller is adopted as shown in Fig. 7. The detailed analysis of proposed control methods is illustrated as follows.

A. Design of Rotor Position Estimator

(1) Quadratic Fit of Position/Time Data by Employing LSPF Algorithm

Given a continuous function $\theta(t)$, which represents the real position, the Hall sensors output a discontinuous quantized position signal θ_h. Hence, with the sensor data $\{(t_1, \theta_{h1}), (t_2, \theta_{h2}), \ldots(t_k, \theta_{hk})\} = \{\text{time, position}\}$, a polynomial approximation to the position with respect to time can be obtained. The LS method is one of the most popular techniques which has been frequently used to calculate the coefficients and to fit data. Thus, the problem of position estimation converts to the problem that finding a polynomial equation that best fits the measured Hall position data.

From the analysis of the average speed method, it can be concluded that the linear fitting is not suitable if speed fluctuations occurs due to the load torque variation or nonlinear speed references.

Generally, it is difficult to choose a proper degree without the pre-knowledge of the position profile. Therefore, to cope with the issue, it is necessary to consider the motion character of a

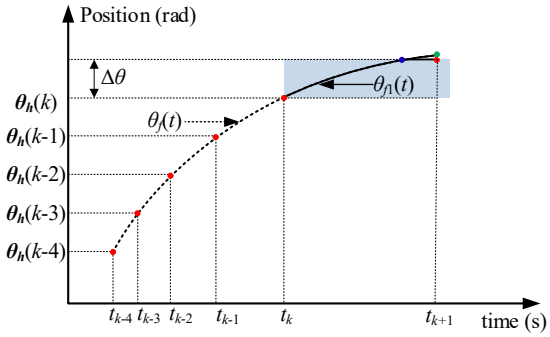

Fig. 8. Fitting strategy. $\theta_f(t)$ is regarded as the reconstruction output at time instant t_k.

motor for servo application [10-13]. Due to the reliability of motor torque control and the constraint of environment uncertainties in servo applications, the degree of the fitting curve is restricted to quadratic as a compromise between accuracy and efficiency, which can be expressed as:

$$\theta_f(t) = a + bt + ct^2 \tag{13}$$

where θ_f is the estimated position and a, b, c are polynomial coefficients.

To reduce the influence of the Hall sensors' inaccuracy, a polynomial fitting approach based on LS algorithm is developed and seven points ($\{(t_{k-6+i}, \theta_{h(k-6+i)}\}$ i=0,1,2,⋯,6) are chosen to do the fitting for there are six Hall states in each electrical period. Therefore, the fitting problem can be formulated by:

$$\underset{\varepsilon}{\text{minimize}} : \varepsilon = \left\| \begin{bmatrix} \theta_f(t_{k-6}) - \theta_{h(k-6)} \\ \vdots \\ \theta_f(t_{k-3}) - \theta_{h(k-3)} \\ \vdots \\ \theta_f(t_k) - \theta_{h(k)} \end{bmatrix} \right\|_2 \tag{14}$$

The coefficients can be solved by setting the derivatives of the minimize function ε with respect to a, b and c. Then, the problem of (14) can be expressed by:

$$\begin{aligned} \frac{d\varepsilon}{da} &= \sum_{i=0}^{6} [\theta_{hi} t_i^2 - (at_i^4 + bt_i^3 + ct_i^2)] = 0 \\ \frac{d\varepsilon}{db} &= \sum_{i=0}^{6} [\theta_{hi} t_i - (at_i^3 + bt_i^2 + ct_i^1)] = 0 \\ \frac{d\varepsilon}{dc} &= \sum_{i=0}^{6} [\theta_{hi} - (at_i^2 + bt_i^1 + c)] = 0 \end{aligned} \tag{15}$$

From (15), the desired polynomial coefficients can be found. With those coefficients, the polynomial function runs continuously to give the estimated position until the beginning of the next Hall sector, say, form t_k to t_{k+1}. If the motor runs forward, as shown in Fig. 8, the next Hall signal will be produced at the position ($\theta_{h(k)}$+ $\Delta\theta$). In addition, in order to gain a better fitting accuracy, a constraint condition is used for the coming Hall sector with θ_f bounded by:

$$\theta_f = \begin{cases} \theta_{h(k)} + \Delta\theta & \text{if } \theta_f \geq \theta_{h(k)} + \Delta\theta \\ \theta_{h(k)} - \Delta\theta & \text{if } \theta_f \leq \theta_{h(k)} - \Delta\theta \\ \theta_f & \text{otherwise} \end{cases} \tag{16}$$

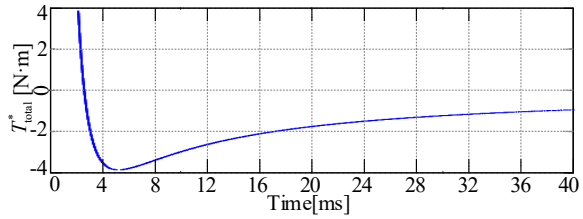

Fig. 9. Relationship of applied torque T^*_{total} and time to travel 60 degrees

To realize a smooth and steady performance at the start-up process, the real-time reconstruction strategy is utilized [22]. As shown in Fig. 7, during the first Hall sector at start-up, the estimated position is described in (17)

$$\hat{\theta}_e = \begin{cases} \theta_h + \dfrac{\pi}{6}, & k = 0 \\ \theta_f \quad , & k \neq 0 \end{cases} \tag{17}$$

(2) Compensation of Position Estimation for Speed Reversal

The proposed LSPF method can estimate the rotor position accurately when motor torque is almost constant during several Hall sectors. Obviously such a condition can be satisfied in most scenarios. Assuming T_{total} as the motor torque and B as the coefficient of friction, the mechanical equation can be written as:

$$J\frac{d^2\theta}{dt^2} = T_{total} + B\frac{d\theta}{dt} \tag{18}$$

As aforementioned, in most cases during several Hall sectors the variation of T_{total} is negligible. Moreover, the friction torque is propositional to speed. During the speed reversal process, indeed the speed is small, therefore the term $Bd\theta/dt$ can be neglected in this certain case. Hence (18) can be solved

$$\theta = c_0 + c_1 t + \frac{T_{total}}{2J}t^2 \tag{19}$$

where c_0 and c_1 are two constants which can be obtained from known positon/time data. Comparing the right-hand side of (13) and (19), gives:

$$c_0 = a, c_1 = b, \frac{T_{total}}{2J} = c \tag{20}$$

However, when the rotor is changing direction, the torque command will have an opposite value, sometimes at a maximum (positive or negative) value [12]. So position estimation error will appear during the Hall sector when the torque command changes. If the torque changes to T^*_{total} at t=0, then (19) is modified after time t=0 to

$$\theta^* = c_0^* + c_1^* t + \frac{T^*_{total}}{J}t^2 \tag{21}$$

The fitting polynomial (13) is updated every 60 electrical degrees $\Delta\theta_h$. So that, with torque T_{total}, the rotor takes t_1 to move distance $\Delta\theta_h$ but with T^*_{total}, the rotor move the same distance in time t_2.

With the information of inertia J as shown in Table I, the relationship of T^*_{total} and the time t_2 that it takes to travel 60 degrees is demonstrated in Fig.9. It is worth to note that when a braking torque is applied (T^*_{total} <0), t_2 has two distinct values,

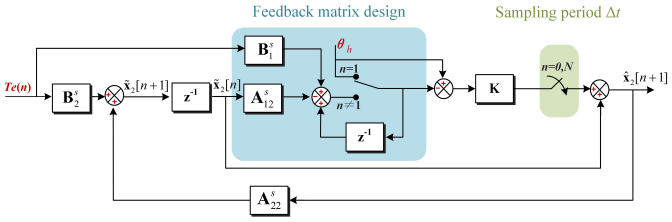

Fig. 10. Block diagram of reduced-order multi-sampling rate observer

which means the rotor will rotate 60 degrees and afterwards reversely move the same positon. However, if the braking torque is too large, the motor will finish the speed reversal within 60 degrees. If we still adopt (13) to estimate position in this case, estimation error will appear. To eliminate the estimation error, (21) should be used instead of (13). To be specific, T^*_{total} comes from the output of speed regulator; while c_1^* and c_2^* are given as follow:

$$\begin{cases} \left.\dfrac{d\theta}{dt}\right|_{t=t_k} = \dfrac{T^*_{total}}{J}\cdot t_k + c_1^* = 2c\cdot t_k + b \\ c_0^* + c_1^* t_k + \dfrac{T^*_{total}}{J}t_k^2 = a + bt_k + ct_k^2 \end{cases} \tag{22}$$

B. Design of speed observer

Traditionally, the whole Hall signal information is used for the estimation of speed and rotor positon. However, it is obvious the Hall position θ_h varies in a step manner, and it only matches with the real rotor position at time instant t_k. Therefore, only θ_h at the verge of Hall signals is valuable and accurate for designing a speed observer. In this paper, the essences of the proposed reduced-order dual-sampling-rate speed observer is to predict the state variables at each control period solely using the θ_h at time instant t_k. The speed observer has a Luenberger structure and is designed on the basis of mechanical dynamics. In addition, the torque reference is applied in the observer as a feedforward term. Fig. 10 demonstrates the block diagram of the proposed speed observer. The detailed design process can be found in [22]. The state space equation of the observer in discrete form is given as follows:

$$\hat{\mathbf{x}}_1[n+1] = \begin{cases} \mathbf{x}_1[n+1], & n = 0 \\ \hat{\mathbf{x}}_1[n] + \mathbf{A}^s_{12}\hat{\mathbf{x}}_2[n] + \mathbf{B}^s_1\mathbf{u}[n], & n = 1,2,...,N-1 \end{cases}$$

$$\hat{\mathbf{x}}_2[n+1] = \begin{cases} \mathbf{A}^s_{22}\hat{\mathbf{x}}_2[n] + \mathbf{B}^s_2\mathbf{u}[n] + \mathbf{K}\{\mathbf{x}_1[n+1] \\ \quad -(\hat{\mathbf{x}}_1[n] + \mathbf{A}^s_{12}\mathbf{x}_2[n] + \mathbf{B}^s_1\mathbf{u}[n])\}, & n = 0 \\ \mathbf{A}^s_{22}\hat{\mathbf{x}}_2[n] + \mathbf{B}^s_2\mathbf{u}[n], & n = 1,2,...,N-1 \end{cases} \tag{23}$$

where $\mathbf{A}^s = \begin{bmatrix} \mathbf{A}^s_{11} & \mathbf{A}^s_{12} \\ \mathbf{A}^s_{21} & \mathbf{A}^s_{22} \end{bmatrix} = \left[\begin{array}{c|cc} 1 & T_s & T_s^2/2\hat{J} \\ \hline 0 & 1 & T_s/\hat{J} \\ 0 & 0 & 1 \end{array}\right]$, $\mathbf{B}^s = \begin{bmatrix} \mathbf{B}^s_1 \\ \mathbf{B}^s_2 \end{bmatrix} = \begin{bmatrix} T_s^2/2\hat{J} \\ T_s/\hat{J} \\ 0 \end{bmatrix}$,

$\mathbf{x}_1$= [θ], $\mathbf{x}_2$=[ω T_L]^T, $\mathbf{u}$ = [T_e], $\mathbf{K}$=[k_1, k_2] is the observer gains.

The selection of proper observer gains is of great importance for the performance of the observer. To maximize performance while limiting errors, pole assignment method is adopted for configuring the observer gains.

The error dynamics can be obtained from (23):

$$\mathbf{e}[k+1] = (\mathbf{A}^{s\ N}_{22} - \mathbf{A}^{s\ N-1}_{22}\mathbf{K}\mathbf{A}^s_{12})\mathbf{e}[k] \tag{24}$$

where $\mathbf{e} = [\mathbf{x}_2 - \hat{\mathbf{x}}_2]$.

Based on (24), the observer gains can be deduced from the

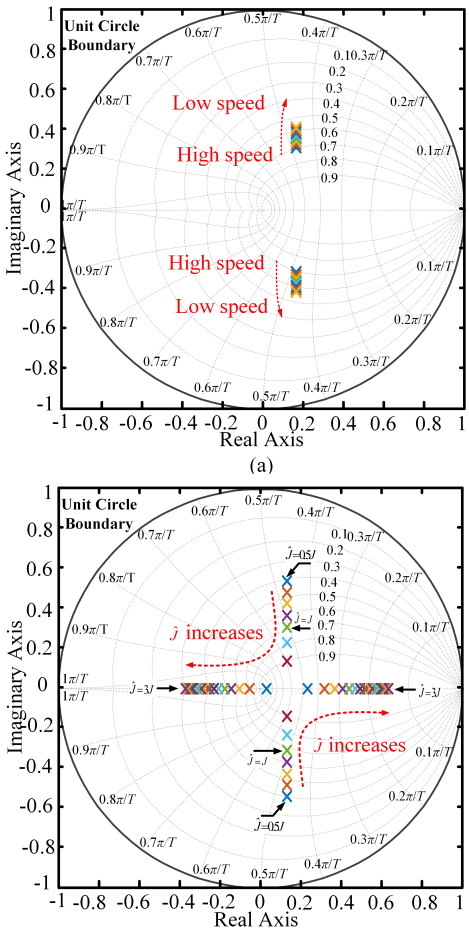

Fig. 11. (a) Movement of the poles in design when speed changes. (b) Poles distribution of the proposed observer as $\hat{J}$ varies

following equation

$$\prod_{i=1}^{2}(z-z_i)=\left|z\mathbf{I}-\mathbf{A}_{22}^{s\ N-1}(\mathbf{A}_{22}^{s}-\mathbf{K}\mathbf{A}_{12}^{s})\right| \tag{25}$$

where z_i denotes the i_{th} desired pole in the unit circle on z-plane.

Eq. (25) can be used for the purpose of pole placement, i.e. as shown in Fig. 11(a), the actual poles of the observer keep inside the unit circle when choosing a constant gain vector. The gain vector is designed with bandwidth 200Hz and damping factor 0.707 at the condition when $\Delta t = 25*T_s$. Also, as shown in Fig. 11(b), the observer maintains the stability even though the mismatch between parameter happens, i.e., the err ΔJ between the actual plant inertia J and the inertia used in the observer, varies from $0.5J$ to $3J$. Therefore, the control system can operate stably with the proposed observer.

V. Experiment Results

For the purpose of demonstrating the effectiveness of the proposed methods, experiments are performed on a test bench (see Fig. 12), and the parameters of the used SPMSM are shown in Table I. To verify the position control ability and mimic the real industrial working condition, a ball screw stage is directly coupled to the shaft of SPMSM. The servo motor is equipped with both a Hall position sensor and an incremental encoder with the resolution of 10000 pluses/rev. The whole control algorithm is implemented with a digital signal processor (DSP) TMS320F28335.

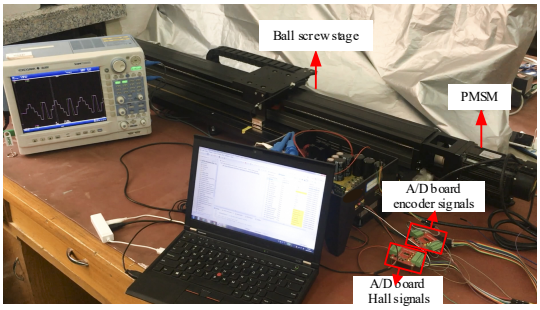

Fig. 12.Experimental platform

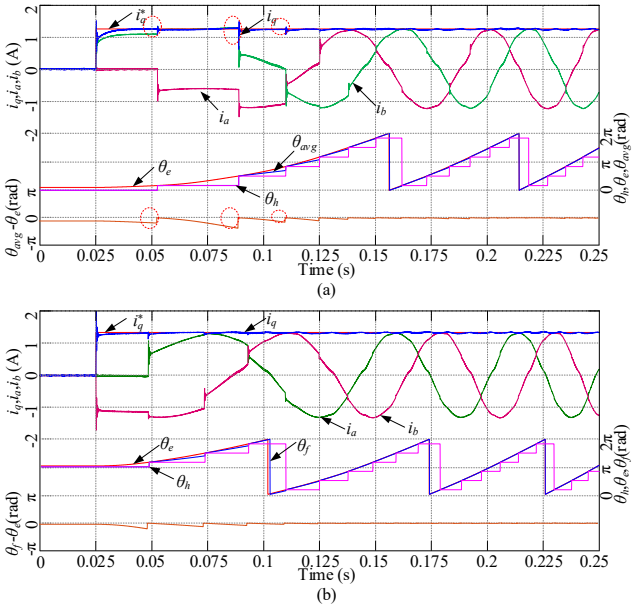

Fig.13. Phase currents and rotor position at startup: a) average speed method. b) proposed LSPF method.

TABLE I. Specification of SPM

Quantity	*Value[Unit]*	*Quantity*	*Value[Unit]*
Pole	8	Stator resistance	2.88[Ω]
Rate torque	2.39[Nm]	Stator inductance	6.4[mH]
Base speed	3000[r/min]	Rotational inertia	0.001638[kg·m^2]
Rated current	3[A]	Voltage constant	48[V/1000r/min]

A. Position estimation performance

Fig. 13 shows the current response in current control mode when the machine rotates from standstill. At the beginning, the stored position/time data is not enough for the estimator to produce a good estimation. When using the average speed method (4) to estimate rotor position, the estimated position can converge to the real position after the rotor travelling first three Hall sectors, as shown in Fig.13 (a), where the maximum instantaneous position error is 60° at the first three Hall sectors during start-up process. Such a position error would deteriorate the torque performance. Since the output torque is proportional to the sine of the position error, therefore maximum possible torque error is (sin(90°) – sin (90°-60°))×100% = 50%. While Fig .13 (b) shows the startup performance when using LSPF method. Compared with Fig.13(a), the position error in Fig.13(b) converges to less than 10° during the second Hall sector due to the proposed real-time reconstruction strategy. From this test, it is clear that the proposed position estimator can effectively start a motor from standstill smoothly and

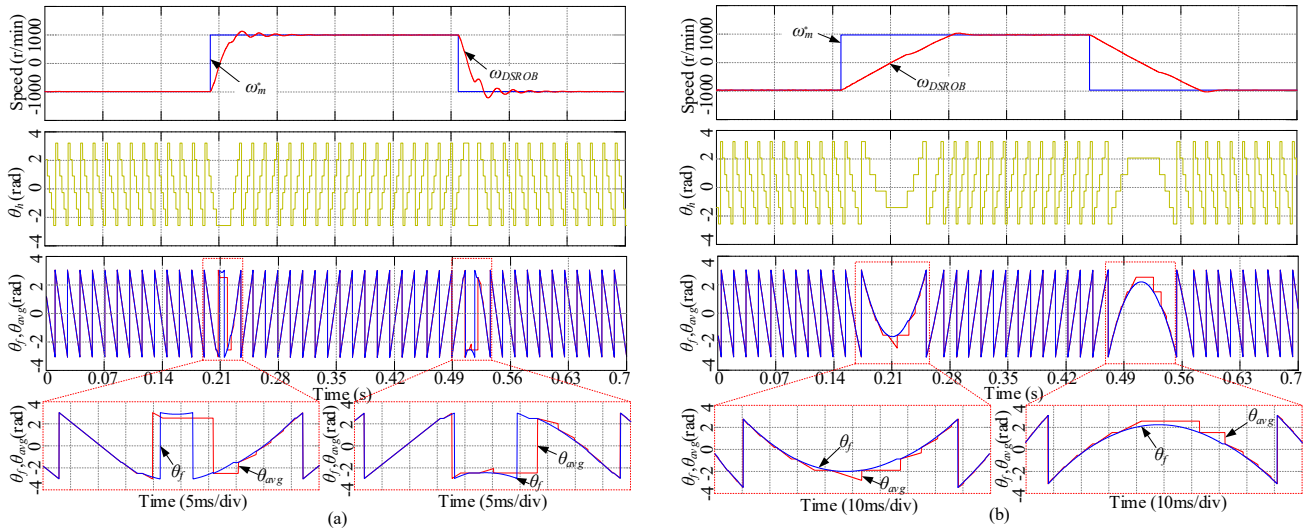

Fig. 14. Position estimation performance at speed reversal process from -1000 r/min to 1000r/min with different system inertia. a) 0.000316 kg·m^2. b) 0.001638 kg·m^2

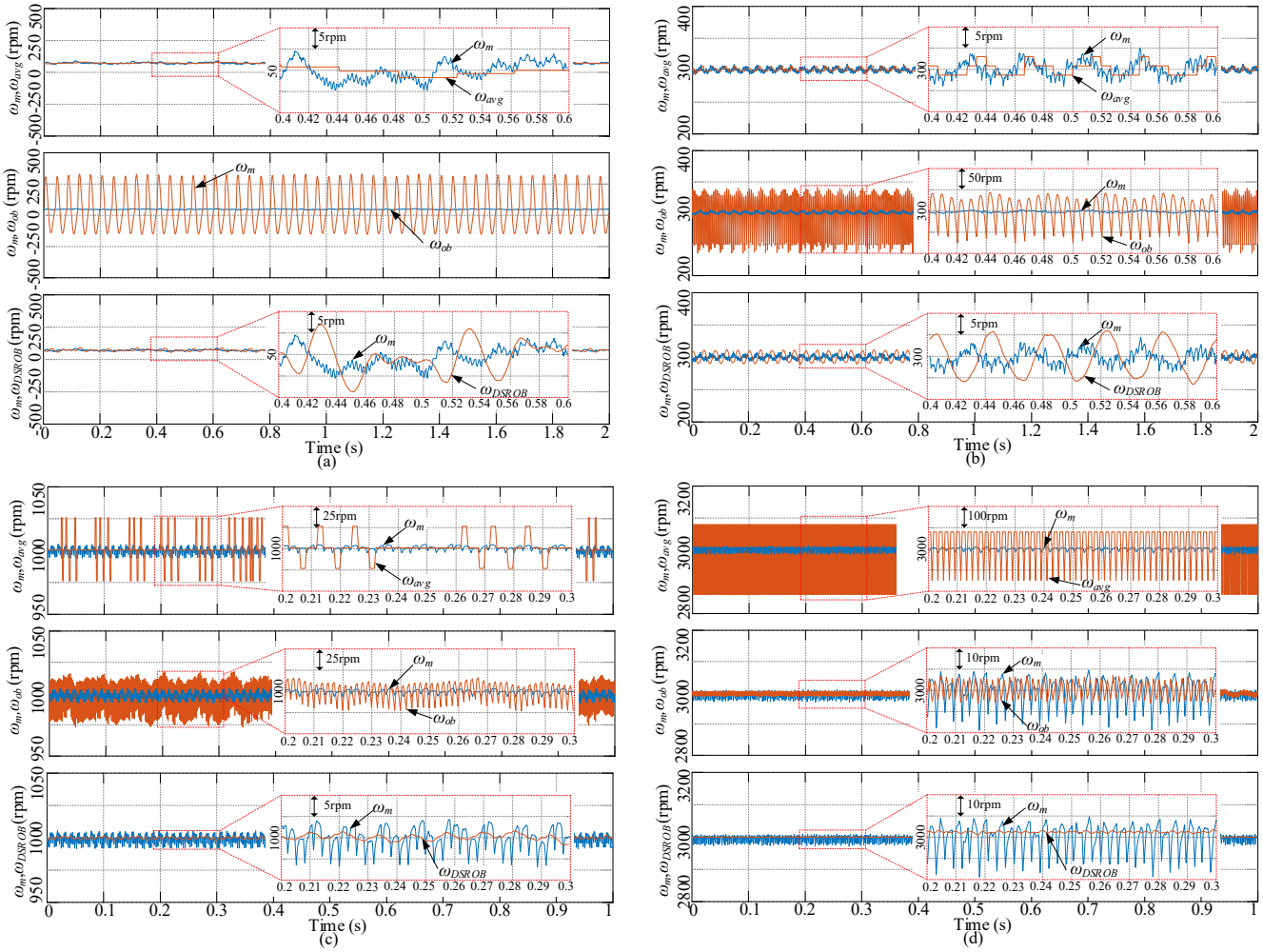

Fig. 15. The speed estimation performances by average speed method, Luenberger observer and proposed dual-sampling-rate observer. a) 50rpm. b) 300rpm. c) 1000rpm. d) 3000rpm

TABLE I COMPARISON OF THE THREE METHODS.

Methods	Peak-to-peak speed ripple (rpm)				Root Mean Squared Error (rpm)			
	50	300	1000	3000	50	300	1000	3000
Average method (rpm)	4.8866	6.7343	50.0313	219.78	2.1544	2.0134	7.9064	99.5111
Luenberger observer (rpm)	518.8857	11.3656	43.5292	25.126	170.4994	30.2259	11.7871	8.2029
Proposed observer (rpm)	16.7364	13.9924	3.9794	2.7288	3.7971	5.6055	2.6598	7.534

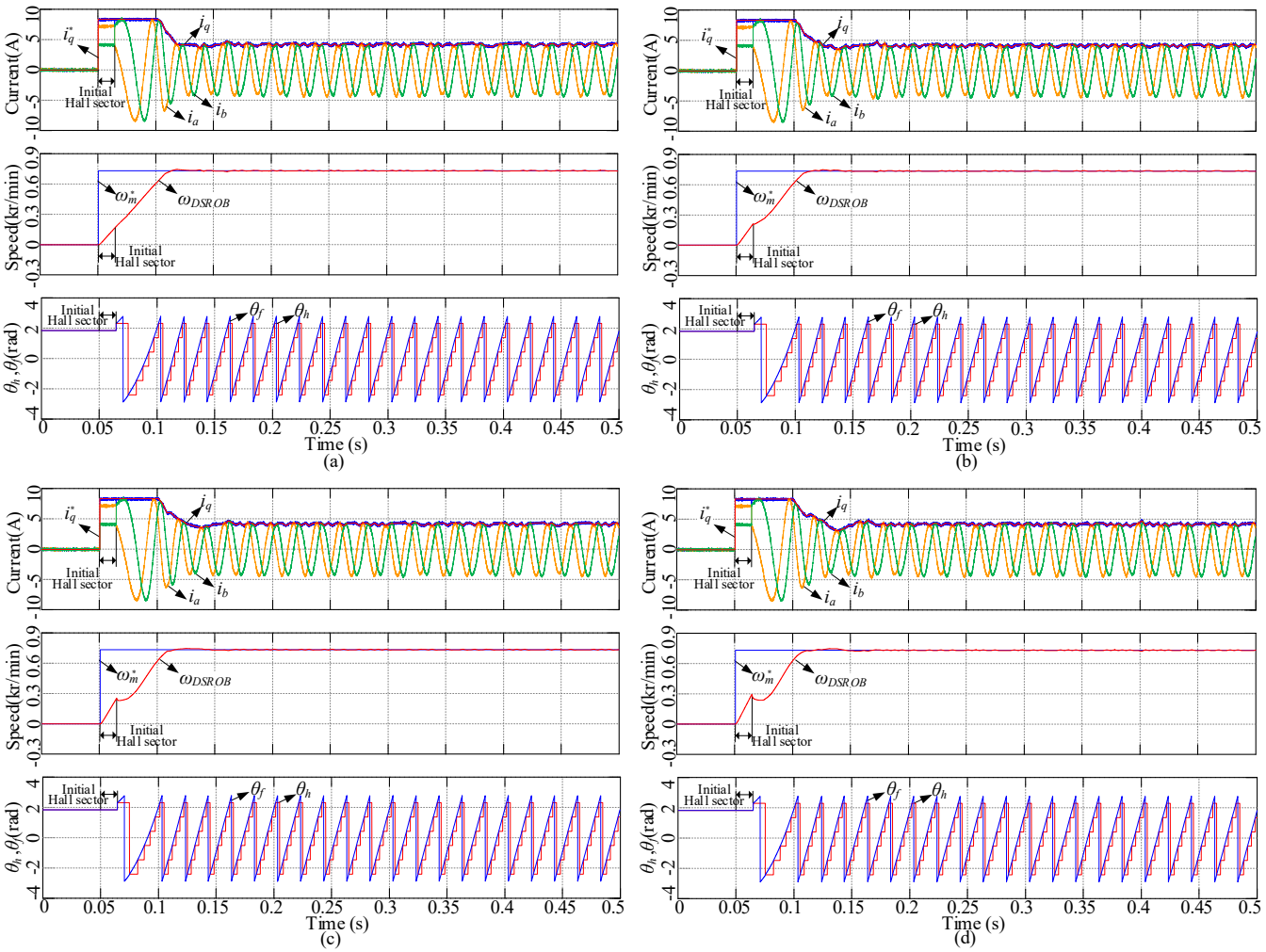

Fig.16. Speed step performance comparison using proposed estimation scheme under full load condition with different $\hat{T}_d(0)$. (a) 100% rated torque. (b) 75% rated torque. (c) 50% rated torque. (d) 25% rated torque

quickly with a desired position estimation performance.

The real position, estimated position using average speed method and proposed LSPF method in speed reversal process under moment of inertia (0.000316 kg·m^2 and 0.001638 kg·m^2) are demonstrated in Fig. 14. As analyzed in Section III-A, it is clear that without the compensation strategy, the estimated position θ_{avg} will increase or decrease monotonously until the next Hall verge recognized even though the actual operation direction has already changed. The estimation error caused by this reason sometimes can be as high as 60°. However, with the proposed LSPF method and compensation scheme, the estimated position θ_f can accurately track the real position θ_e, validating that the proposed position estimator has good estimation accuracy during the whole reversal process, besides, it can be seen the compensation method is still validate in fast dynamic condition as shown in Fig.14 (a).

B. Speed estimation performance

Fig. 15 shows the speed estimation performance when motor is running at 50r/min, 300r/min, 1000r/min and 3000r/min, respectively. Again, θ_e: is the real position. θ_f: is the estimated position using proposed LSPF method. θ_{avg}: the estimated position using average speed method. θ_h: position generated from Hall signals. ω_m: mechanical angular speed obtained from the shaft incremental encoder. The waveforms from top to bottom are speed estimation using average speed method (ω_{avg}), Luenberger observer (LOB, ω_{ob}) and proposed dual-sampling-rate observer (DSROB, ω_{DSROB}). It can be seen that the speed estimation error of average speed method is roughly linear with actual speed, which is consistent with equation (3). The estimated speed of LOB has obvious oscillation especially in low speed region, which is caused by the discontinuity of LOB input. This can be explained that as the decrease of speed, the sampling rate of Hall sensor will decrease as well, leading to the deteriorated performance of LOB method. In order to better illustrate the performance comparison using different methods in Fig. 15, root mean squared error and peak-to-peak speed ripple are concluded in Table II.

However, with the proposed DSROB, the influence of discontinuous effect of input is weakened due to the dual-sampling character of proposed observer. This explains why the estimated speed of DSROB is much smoother compared with LOB.

In order to test the performance of the proposed method under the loading condition, full load is added under the start-up, and results are shown in Fig. 16.

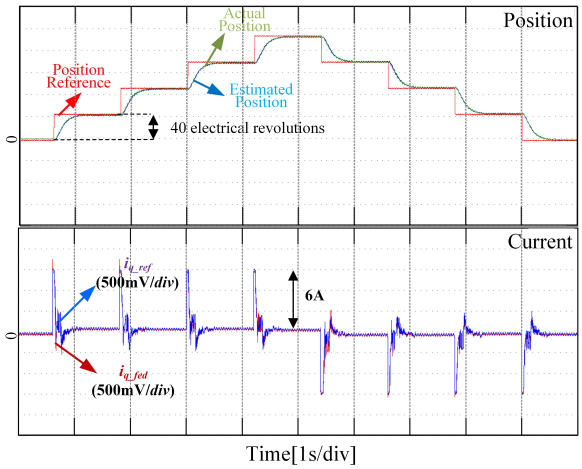

Fig. 17. Position loop control performance with proposed approach

Fig. 16 (a), (b), (c) and (d) are the experiment results of motor start-up at full load when default load ($\hat{T}_d(0)$) setting in the speed observer are 100 %, 75 %, 50 % and 25 % of the rated load, respectively (speed reference is 750rpm step speed). To evaluate the performance under the worst standstill condition, the initial position is set to be the middle of a specific Hall sector (which will cause maximum 30 electrical degrees error).

It can be seen from Fig. 16 that the loading condition provides negligible influence to position estimation and current-loop control. Such results are due to the fact that the proposed position estimator is a non-model based estimator, so the performance is invulnerable to system mechanism characters, the results meet the aforementioned theoretical analysis. The loading condition will influence the speed estimation, especially when big difference between $\hat{T}_d(0)$ and T_d occurs (Fig. 16 (d)).

C. *Position loop control performance*

To verify the feasibility of proposed idea in the positioning application, the position control experiment is carried out as shown in Fig.17. The position reference is given in a step manner. The actual position which is obtained from a 10,000 pluses/rev encoder, the estimated position from proposed method, and the q-axis currents are exhibited. It can be seen from Fig. 17, the proposed scheme can realize position control, and the position accuracy is within 30 electrical degrees. Considering the number of pole pairs (p=4), shaft diameter (19mm) and the lead of ball screw (20), the position error in the linear side is smaller than 0.416mm. Therefore, this accuracy is sufficient to satisfy many industrial applications for position control requirement such as auto door, conveyer belt, packing machine and so on.

VI. CONCLUSION

In this paper, the drawbacks of conventional non-model-based and model-based position/speed estimation methods in practical applications are analyzed. To exploit the advantages and avoid the drawbacks of each method, an improved approach is proposed, in which the model-free method is for position estimation and model-based method is for speed estimation. Besides, suitable compensation ideas are proposed and performed into practical test system, confirming a desired performance within a wide speed range. The feasibility and effectiveness of the proposed method is verified by experiments. Experimental results show that compared with the conventional methods, the proposed scheme is able to smoothly manage the speed and position estimation. However, the Hall position sensors based motor drive also has its limitations, such as it cannot realize precise position control, and it is vulnerable to load disturbance. Experimental results highlight this promising method in the low cost applications which require position control.

REFERENCES

[1] Z. Chen, J. Gao, F. Wang, Z. Ma, Z. Zhang, and R. Kennel, "Sensorless control for SPMSM with concentrated windings using multisignal injection method," *IEEE Trans. Ind. Electron.*, vol. 61, no. 12, pp. 6624–6634, 2014..

[2] S. Murakami, T. Shiota, M. Ohto, K. Ide, and M. Hisatsune, "Encoderless servo drive with adequately designed IPMSM for pulse-voltage-injection-based position detection," *IEEE Trans. Ind. Appl.*, vol. 48, no. 6, pp. 1922–1930, 2012.

[3] S. K. Sul, Y. Kwon, and Y. Lee, "Sensorless control of IPMSM for last 10 years and next 5 years," *CES Trans. Electr. Mach. Syst.*, vol. 1, no. 2, pp. 91–99, 2017.

[4] L. Rovere, A. Formentini, A. Gaeta, P. Zanchetta, and M. Marchesoni, "Sensorless Finite-Control Set Model Predictive Control for IPMSM Drives," *IEEE Trans. Ind. Electron.*, vol. 63, no. 9, pp. 5921–5931, 2016.

[5] Y. C. Kwon, S. K. Sul, N. A. Baloch, S. Morimoto, and M. Ohto, "Design, modeling, and control of an IPMSM with an asymmetric rotor and search coils for absolute position sensorless drive," *IEEE Trans. Ind. Appl.*, vol. 52, no. 5, pp. 3839–3850, 2016.

[6] M. C. Harke, G. C. De Donato, F. G. Capponi, T. R. Tesch, and R. D. Lorenz, "Implementation issues and performance evaluation of sinusoidal, surface-mounted PM machine drives with hall-effect position sensors and a vector-tracking observer," *IEEE Trans. Ind. Appl.*, vol. 44, no. 1, pp. 161–173, 2008.

[7] S. Zaim, J. P. Martin, A. H. Effect, and P. Sensor, "High Performance Low Cost Control of a Permanent Magnet Wheel Motor Using a Hall Effect Position Sensor," *2011 IEEE Veh. Power Propuls. Conf.*, pp. 1–6, 2011.

[8] S. B. Ozturk, O. C. Kivanc, B. Atila, S. U. Rehman, B. Akin, and H. A. Toliyat, "A simple least squares approach for low speed performance analysis of indirect FOC induction motor drive using low-resolution position sensor," *2017 IEEE Int. Electr. Mach. Drives Conf. IEMDC 2017*, pp. 1–8, 2017.

[9] H. J. Ahn and D. M. Lee, "A New Bumpless Rotor-Flux Position Estimation Scheme for Vector-Controlled Washing Machine," *IEEE Trans. Ind. Informatics*, vol. 12, no. 2, pp. 466–473, 2016.

[10] L. Chen, M. Laffranchi, N. G. Tsagarakis, and D. G. Caldwell, "A novel curve fitting based discrete velocity estimator for high performance motion control," *IEEE/ASME Int. Conf. Adv. Intell. Mechatronics, AIM*, pp. 1060–1065, 2012.

[11] L. Bascetta, G. Magnani, and P. Rocco, "Velocity Estimation : Assessing the Performance of," *Control*, vol. 17, no. 2, pp. 424–433, 2009.

[12] Z. Feng and P. P. Acarnley, "Extrapolation technique for improving the effective resolution of position encoders in permanent-magnet motor drives," *IEEE/ASME Trans. Mechatronics*, vol. 13, no. 4, pp. 410–415, 2008.

[13] H. Zhu, T. Sugie, and H. Fujimoto, "Smooth output reconstruction for linear systems with quantized measurements," *Asian J. Control*, vol. 17, no. 3, pp. 1039–1049, 2015.

[14] G. De Donato, G. Scelba, M. Pulvirenti, G. Scarcella, and F. Giulii Capponi, "Low-Cost, High-Resolution, Fault-Robust Position and Speed Estimation for PMSM Drives Operating in Safety-Critical Systems," *IEEE Trans. Power Electron.*, vol. 34, no. 1, pp. 550–564, 2018.

[15] L. Kovudhikulrungsri and T. Koseki, "Precise speed estimation from a low-resolution encoder by dual-sampling-rate observer," *IEEE/ASME Trans. Mechatronics*, vol. 11, no. 6, pp. 661–670, 2006.

[16] G. Scelba, G. De Donato, G. Scarcella, F. Giulii Capponi, and F. Bonaccorso, "Fault-tolerant rotor position and velocity estimation using binary hall-effect sensors for low-cost vector control drives," *IEEE Trans. Ind. Appl.*, vol. 50, no. 5, pp. 3403–3413, 2014.

[17] A. Yoo, S. Sul, D. Lee, and C. Jun, "Novel Speed and Rotor Position Estimation Strategy Using a Dual Observer for Low-Resolution Position Sensors," *Ieee Trans. Power Electron.*, vol. 24, no. 12, pp. 2897–2906, 2009.

[18] S. Y. Kim, C. Choi, K. Lee, and W. Lee, "An improved rotor position estimation with vector-tracking observer in PMSM drives with low-resolution hall-effect sensors," *IEEE Trans. Ind. Electron.*, vol. 58, no. 9, pp. 4078–4086, 2011.

[19] J. B. Kim and B. K. Kim, "Development of Precise Encoder Edge-Based State Estimation for Motors," *IEEE Trans. Ind. Electron.*, vol. 63, no. 6, pp. 3648–3655, 2016.

[20] T. Shi, Z. Wang, and C. Xia, "Speed Measurement Error Suppression for PMSM Control System Using Self-Adaption Kalman Observer," *IEEE Trans. Ind. Electron.*, vol. 62, no. 5, pp. 2753–2763, 2015.

[21] K. Ohishi, Y. Ogawa, and H. Dohmaki, "A Speed Control Method for a PM Motor Using a Speed Observer and a Low-Resolution Encoder," vol. 143, no. 1, pp. 209–216, 2003.

[22] Q. Ni, M. Yang, et al. " Analysis and Design of Position and Velocity Estimation Scheme for PM servo motor drive with Binary Hall Sensors." *IEEE Energy Conversion Congress and Exposition* (ECCE), Portland, OR, 2018

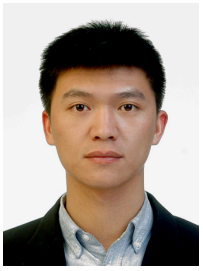

Qinan Ni received the B.S. degree in electrical engineering from Nanjing University of Information Science and Technology, Nanjing, China, in 2013, and M.S. degrees in electrical engineering from Harbin Institute of Technology, Harbin, China, in 2015, where he is currently working toward Ph.D. degree in power electronics and electrical drives at the School of Electrical Engineering and Automation. From 2017 to 2018, he was a Visiting Student in PEMC Group at University of Nottingham.

His current research interests include advanced control of permanent magnet synchronous motor drives and position sensor-less control of ac motors.

Ming Yang (M'14, SM'18) received the B.S. and M.S. and Ph.D. degrees in Electrical Engineering from Harbin Institute of Technology, Harbin, China, in 2000, 2002 and 2007, respectively.

In 2004, he joined the Department of Electrical Engineering, HIT as a Lecturer, where he has been an Associate Professor of Electrical Engineering since 2010. From 2009 to 2012, he was a Postdoctoral Fellow in Shanghai STEP Electric Corporation. He has authored more than 40 technical papers published in journals and conference proceedings. He is the holder of fourteen Chinese patents. His current major research interests include PMSM servo system, predictive current control, mechanical resonance suppression and gear fault detection based on motor drive systems.

Shafiq A. Odhano (S'13–M'15) received the M.Sc. degree in electrical engineering and the Ph.D. degree in power electronics, machines and drives from the Politecnico di Torino, Turin, Italy, in 2014. He was a Post-Doctoral Research Fellow with the Politecnico di Torino. He is currently a Post-Doctoral Research Fellow with the University of Nottingham, Nottingham, U.K. His current research interests include high-performance control of servodrives, model predictive control of power converters, and self-commissioning of ac motor drives. Dr. Odhano was a recipient of the IEEE-IAS Prize Paper Award in 2015.

Mi Tang was born in Chengdu, Sichuan, China, in 1990. She received her M.Sc. degree in Electrical Engineering and Ph.D. degree in Electrical and Electronic Engineering from the University of Nottingham, Nottingham, UK, in 2012 and 2017 respectively. She is currently working as a Research Fellow at the Power Electronics and Machine Control Group at the University of Nottingham, Nottingham, UK. Her research interests include dead beat control and repetitive control.

Pericle Zanchetta (M'00, SM'15, F'18) received the M. Eng. degree in electronic engineering and the Ph.D. degree in electrical engineering from the Technical University of Bari (Italy) in 1993 and 1997, respectively. In 1998, he became Assistant Professor of power electronics at the same university. In 2001, he became a Lecturer in control of power electronics systems in the PEMC Research Group, University of Nottingham, U.K., where he is currently a Professor. He has authored or coauthored more than 300 peer-reviewed papers. His research interests include control and optimization of power converters and drives, matrix and multilevel converters. Prof. Zanchetta has been Chair of the IEEE-IAS Industrial Power Converter Committee (IPCC) and is now transactions review chair for IPCC. He is also Vice Chair of the IEEE-IAS Industrial Power Conversion Systems Department (IPCSD).

Xiaosheng Liu was born in Qiqihaer, China, in 1966. He received the bachelor's degree(in 1988), master's degree(in 1993) and doctor's degree(in 1999) from Harbin Institute of Technology(HIT), Harbin, China. Now he is a professor in the Department of Electrical Engineering, HIT. His main interests and research fields include power line communication and its routing methods, communication networks & control technology, information and communication of Smart grids, and electrical motor drives.

Dianguo Xu (M'97, SM'12, F'17) received the B.S. degree in Control Engineering from Harbin Engineering University, Harbin, China, in 1982, and the M.S. and Ph.D. degrees in Electrical Engineering from Harbin Institute of Technology, Harbin, China, in 1984 and 1989, respectively.

In 1984, he joined the Department of Electrical Engineering, HIT as an assistant professor. Since 1994, he has been a professor in the Department of Electrical Engineering, HIT. He was the Dean of School of Electrical Engineering and Automation, HIT from 2000 to 2010. He is now the Vice President of HIT. His research interests include renewable energy generation, power quality mitigation, sensorless motor drives, and high performance servo system. Dr. Xu is a Fellow of IEEE, and an Associate Editor of the IEEE TRANSACTIONS ON INDUSTRIAL ELECTRONICS.